

Magnetotransport in the $\text{La}_{1.2}(\text{Sr}, \text{Ca})_{1.8}\text{Mn}_2\text{O}_7$ solid solution

This article has been downloaded from IOPscience. Please scroll down to see the full text article.

2002 J. Phys.: Condens. Matter 14 6667

(<http://iopscience.iop.org/0953-8984/14/26/307>)

View [the table of contents for this issue](#), or go to the [journal homepage](#) for more

Download details:

IP Address: 171.66.16.96

The article was downloaded on 18/05/2010 at 12:11

Please note that [terms and conditions apply](#).

Magnetotransport in the $\text{La}_{1.2}(\text{Sr}, \text{Ca})_{1.8}\text{Mn}_2\text{O}_7$ solid solution

M Velázquez^{1,2,4,5}, J M Bassat³, J P Renard², C Dupas² and A Revcolevschi¹

¹ Laboratoire de Physico-Chimie de l'Etat Solide, Université de Paris-Sud, UMR 8648, 91405 Orsay Cedex, France

² Institut d'Electronique Fondamentale, Université de Paris-Sud, UMR 8622, 91405 Orsay Cedex, France

³ Institut de Chimie de la Matière Condensée de Bordeaux-CNRS, 33608 Pessac, France

E-mail: matvel@chem.nwu.edu

Received 5 February 2002

Published 21 June 2002

Online at stacks.iop.org/JPhysCM/14/6667

Abstract

High-quality single crystals of $\text{La}_{1.2}\text{Sr}_{1.8-y}\text{Ca}_y\text{Mn}_2\text{O}_7$ ($0 \leq y \leq 0.2$) were studied by means of electrical resistivity and magnetoresistance measurements. They exhibit a phase transition to a metallic ferromagnetic state at low temperature and strongly anisotropic electronic transport properties, which result from their lamellar structure. The temperature range of the resistivity measurements is extended up to about 1000 K, which allows us to discriminate between different theoretical models. In addition, an accurate comparison of parallel and perpendicular resistivity is carried out in order to reveal the effect of the two-dimensional magnetic correlations. The effect of disorder achieved by substitution of Ca^{2+} , of smaller ionic radius, for Sr^{2+} is also investigated in detail.

1. Introduction

The layered manganites of general formula $\text{La}_{2-2x}\text{Sr}_{1+2x}\text{Mn}_2\text{O}_7$ with $0.3 \leq x \leq 0.5$ exhibit remarkably rich physical properties, that stem from the great intricacy of the orbital, lattice, charge and spin degrees of freedom [1, 2]. Moritomo *et al* [1] first unveiled, in $\text{La}_{1.2}\text{Sr}_{1.8}\text{Mn}_2\text{O}_7$, a reversible insulator–metal transition and a maximum magnetoresistance (MR) $\text{MR}_{max} = (\rho(0 \text{ T}) - \rho(7 \text{ T}))/\rho(7 \text{ T}) \approx 199$ at $T(\text{MR}_{max}) = 129 \text{ K}$, associated with a paramagnetic–ferromagnetic transition at $T_C = 126 \text{ K}$, as well as strongly anisotropic electrical resistivity. These quasi-2D $n = 2$ manganites also are, from the point of view of the electronic behaviour, at the boundary between the perovskites $(\text{La}, \text{Sr})\text{MnO}_3$ ($n \rightarrow \infty$) and the $n = 1$ variety

⁴ Author to whom any correspondence should be addressed.

⁵ Present address: Northwestern University, Department of Chemistry, 2145, N Sheridan Road, 60208-3113 Evanston, IL, USA.

(La, Sr)₂MnO₄ (K₂NiF₄ structure). Whereas the former exhibit a metallic character beyond a certain strontium content, with a finite density of states at the Fermi level $n(E_F)$, the (La, Sr)₂MnO₄ manganites possess a gap in the density of states $n(E)$ at E_F , rendering all of them insulating. The La_{1.2}Sr_{1.8}Mn₂O₇ band structure, recently investigated [3], is characterized by a vanishingly small spectral weight at E_F , making a forecast concerning its metallic and/or insulating nature delicate. The absence of thermal hysteresis was also observed in high-pressure resistivity measurements [4]. Furthermore, several studies [5] have shown that the three different Mn–O distances in this compound vary rapidly but continuously with temperature near the insulator–metal transition, clearly indicating the second-order character of the transition. The magnetic phase diagram in the vicinity of the nominal composition La_{1.2}Sr_{1.8}Mn₂O₇ is still controversial [6]. Some authors claim that it undergoes a second-order ferromagnetic transition at $T_C = 116$ K, resulting in a slightly canted uniform phase, while according to other researchers, ferromagnetic and antiferromagnetic phases could coexist at this composition. The transport anisotropy results from the structure, consisting of magnetic Mn bilayers parallel to the *ab*-plane, separated from each other by a non-magnetic (La, Sr)O layer. This confers a 2D character to the magnetism leading to relatively low T_C -values and to spin correlations extending well above T_C [7], although the ferromagnetic transition is induced by the small exchange interaction between the adjacent Mn bilayers [8].

In this paper, we present an extensive study of the transport and magnetotransport properties of high-quality single crystals of La_{1.2}(Sr, Ca)_{1.8}Mn₂O₇. With respect to previous similar investigations on La_{1.2}Sr_{1.8}Mn₂O₇, the temperature range of resistivity measurements is extended to temperatures up to about 1000 K, which allows us to discriminate between different theoretical models. In addition, an accurate comparison of parallel and perpendicular resistivity is carried out in order to reveal the effect of the 2D magnetic correlations. Finally, we shall consider the effect of disorder achieved by substitution of Ca²⁺, of smaller ionic radius, for Sr²⁺ in detail.

2. Experimental procedure

The growth of La_{1.2}Sr_{1.8-y}Ca_yMn₂O₇ ($0 \leq y \leq 0.2$) single crystals, by the floating zone method associated with an image furnace, along with chemical, crystallographic and microstructural characterizations, were reported in detail elsewhere [9]. Electrical resistivity measurements were made by the standard four-probe technique using typically $2 \times 4 \times 8$ mm³ oriented single crystals at temperatures varying from 2 to 300 K. 50 μm gold wires were fixed by means of a slowly drying silver paint. In order to enable the latter to wet the cleaved surface better, metallic tracks were pre-sputtered (a 100 Å thick Cr one covered by a 1000 Å thick Au one). A magnetic field varying up to 10 T, supplied by a superconducting coil, allowed MR measurements, all performed with the current injected parallel to the magnetic field, itself always applied parallel to the crystallographic direction. High-temperature measurements were carried out in air from 300 to 1000 K, with the same heating and cooling rates (8 mK s⁻¹) as those used in the 2–300 K resistivity measurements. The sample was fixed on an alumina rod and the contacts, attached with Pt paint, underwent a further annealing after deposition.

3. Results and discussion

3.1. High-temperature resistivity of La_{1.2}Sr_{1.8}Mn₂O₇

Figure 1 shows the temperature dependence of the parallel (current along [110]) and perpendicular (current along [001]) resistivity of La_{1.2}Sr_{1.8}Mn₂O₇ from $T_{im} \approx 128$ K up

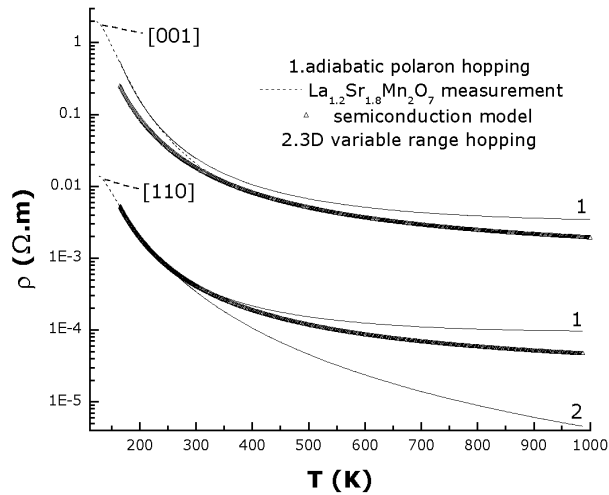


Figure 1. High-temperature resistivity of $\text{La}_{1.2}\text{Sr}_{1.8}\text{Mn}_2\text{O}_7$. The parallel resistivity data fit to a semiconduction law so well that the resulting non-linear least-squares fit merges with the measurements.

to 1000 K $\sim 7.7T_{im}$. We also plotted the non-linear least-squares best fits between the measurements and the theoretical predictions of textbook models. The experimental data for the parallel resistivity fit very well the classical semiconduction law, $\rho = \rho_0 \exp(-E_{act}/k_B T)$ in the 165–1000 K temperature domain, with $\rho_0 \approx 2 \times 10^{-5} \Omega \text{ m}$ and $E_{act}/k_B \approx 937.2 \text{ K} \sim 1.07\hbar\omega_0/k_B$ (ω_0 being the most energetic optical phonon frequency [10]). In contrast, the polaron and variable-range hopping models satisfactorily fit the data only in a restricted temperature range ($\leq 300 \text{ K}$). In the same 165–1000 K range, the semiconduction and adiabatic polaron hopping models do not fit the perpendicular resistivity data even reasonably well. On restricting the temperature range to 400–1000 K, a reasonable fit to the classical semiconduction law with $\rho_0 \approx 7.3 \times 10^{-4} \Omega \text{ m}$ and $E_{act}/k_B \approx 961.3 \text{ K}$ is obtained, but this law clearly departs from experimental data at lower temperature. This difference in temperature dependence between the perpendicular and parallel resistivity clearly shows the effect of the non-magnetic (La, Sr)O barriers.

The anisotropy ratio, $\rho_{[001]}/\rho_{[110]}$, for $\text{La}_{1.2}\text{Sr}_{1.8}\text{Mn}_2\text{O}_7$ varies from ≈ 54 at room temperature to ≈ 214 at $\approx 120 \text{ K}$ (figure 2). This large increase is probably due to there being stronger spin correlations in the ab -plane than along the c -direction with lowering temperature. At temperatures higher than $\sim 425 \text{ K}$, this ratio becomes nearly constant, in agreement with the observed mean-field magnetic behaviour in all directions [8], which reflects the absence of significant spin correlations in this temperature range. On the other hand, once the magnetic moments are all almost perfectly aligned in all directions well below the Curie temperature, the $\rho_{[001]}/\rho_{[110]}$ ratio again reaches a constant value of ≈ 60 . Interestingly, in $\text{La}_{1.2}\text{Sr}_{1.6}\text{Ca}_{0.2}\text{Mn}_2\text{O}_7$, the remarkable result is a strong reduction in resistivity anisotropy at low temperatures, with $\rho_{[001]}/\rho_{[110]} \approx 4$.

At 300 K, that is $\sim 2.8T_C$, there remains a MR(8 T) of ≈ 0.2 for all compositions and in all directions. This effect, of much lower magnitude than that exhibited by perovskites, whose Curie point lies near room temperature, is probably related to the existence of weak quasi-two-dimensional magnetic fluctuations at ambient temperature. The latter appear, for instance, at about 420 K for $\text{La}_{1.2}\text{Sr}_{1.8}\text{Mn}_2\text{O}_7$ [8].

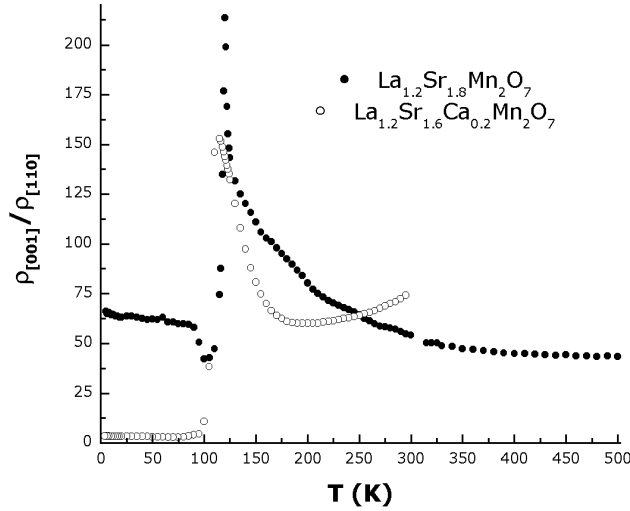


Figure 2. Resistivity anisotropy ratio, $\rho_{[001]}/\rho_{[110]}$, of $\text{La}_{1.2}\text{Sr}_{1.8}\text{Mn}_2\text{O}_7$ and $\text{La}_{1.2}\text{Sr}_{1.6}\text{Ca}_{0.2}\text{Mn}_2\text{O}_7$, as a function of temperature.

3.2. Resistivity and magnetoresistance in the vicinity of the insulator–metal transition

The insulator–metal transition of $\text{La}_{1.2}\text{Sr}_{1.8}\text{Mn}_2\text{O}_7$ occurs reversibly at $T_{im} \approx 128 \text{ K} \sim \theta_D/2$ [11], higher than $T_C \approx 108 \text{ K}$ [8]. If we rely exclusively on the resistivity slope sign criterion, the e_g electron delocalization happens along the c -axis for all compounds (figure 3), consistently with the three-dimensional nature of the ferromagnetic ordering. However, the conclusion is completely different when using the Ioffe–Regel criterion for metallicity, $\rho < 2\pi\hbar c/(4e^2) \approx 8 \times 10^{-3} \Omega \text{ cm}$, which expresses the fact that the mean free path exceeds the distance between two neighbouring atoms. In the present case, this inequality is fulfilled, and thus the metallicity established, only within the perovskite blocks of $\text{La}_{1.2}\text{Sr}_{1.8}\text{Mn}_2\text{O}_7$ and at low temperatures. This is probably related to the fact that the ferromagnetic couplings within the perovskite slabs are two orders of magnitude higher than those between the bilayered blocks [12]. Indeed, in the double-exchange model, the ferromagnetic coupling between two Mn cations is proportional to the transfer integral of the e_g electron between these cations and, thus, it is not surprising that the parallel resistivity is also about two orders of magnitude smaller than the perpendicular one.

Ca doping reduces T_{im} to $\approx 104 \text{ K}$ for $\text{La}_{1.2}\text{Sr}_{1.6}\text{Ca}_{0.2}\text{Mn}_2\text{O}_7$ and clearly shifts the resistivity towards higher values, as shown in figure 3. The values of the resistivity at the insulator–metal transition temperature remain much higher than those of perovskites with similar hole concentration [13]. The abrupt drop in resistivity just below T_{im} (figure 3) does not fit conventional models (neither $\propto T^2$ nor $\propto T \exp(T/\theta_D)$ functional forms). Even in the range of smoother variation $\sim 50\text{--}75 \text{ K}$, fits to a $\rho_0 + aT^\alpha$ type of law yield unexpected exponents $\alpha > 6$ for all compositions and in all directions. In any case, figure 4 strongly suggests that the insulator–metal transition takes place when the magnetic correlation length starts to diverge, which means that the delocalization of the e_g electron occurs when the spins of Mn neighbours in perovskite bilayered blocks become almost parallel. The strong 2D spin correlations in $\text{La}_{1.2}\text{Sr}_{1.8}\text{Mn}_2\text{O}_7$ explain why the temperature of maximum resistivity is significantly larger than the Curie temperature for this manganite, whereas these temperatures are close together for 3D perovskite materials.

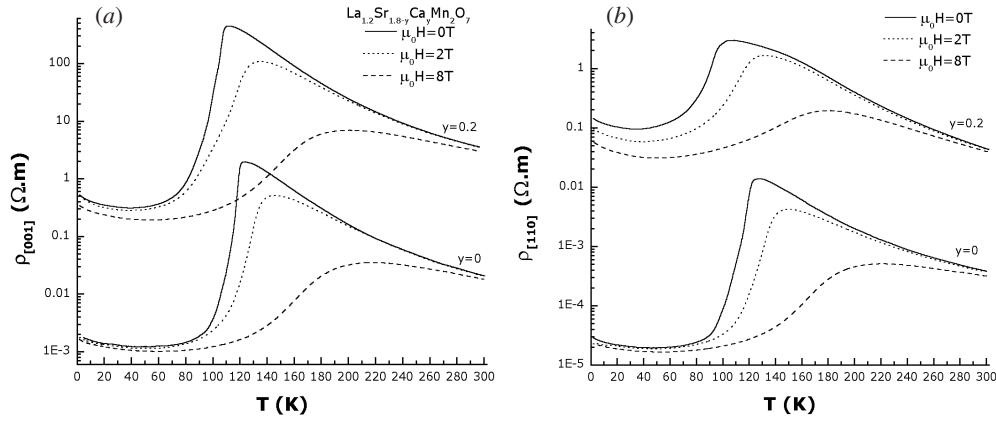


Figure 3. Perpendicular (a) and parallel (b) resistivity of $\text{La}_{1.2}\text{Sr}_{1.8}\text{Mn}_2\text{O}_7$ and $\text{La}_{1.2}\text{Sr}_{1.6}\text{Ca}_{0.2}\text{Mn}_2\text{O}_7$ single crystals, as a function of temperature under various applied magnetic fields.

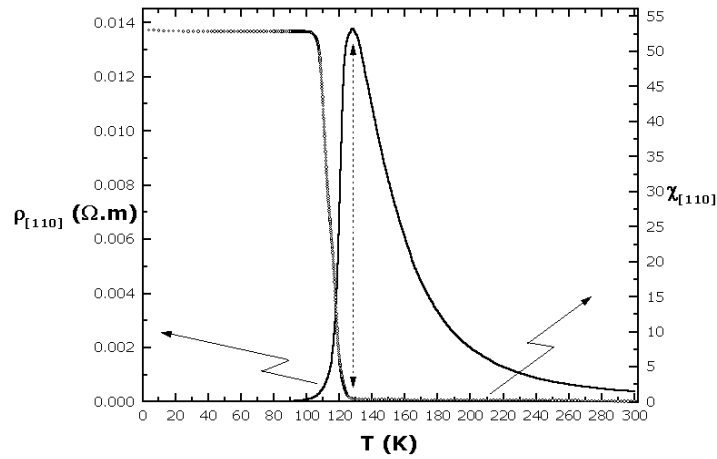


Figure 4. The transport-magnetism correlation in $\text{La}_{1.2}\text{Sr}_{1.8}\text{Mn}_2\text{O}_7$. The magnetic susceptibility measured under 1.48 mT is taken from [8].

High-field MR values produced at the insulator-metal transition are indeed present in the $\text{MR}_{\text{max}} = ((\rho(0) - \rho(\mu_0 H)) / \rho(\mu_0 H))_{\text{max}}$ versus T_C curve drawn for polycrystalline manganese perovskites by Khazeni *et al* [14] ($\text{MR}_{\text{max}[110]}(8 \text{ T}) \approx 500$ for $\text{La}_{1.2}\text{Sr}_{1.8}\text{Mn}_2\text{O}_7$ and $\text{MR}_{\text{max}[110]}(8 \text{ T}) \approx 60$ for $\text{La}_{1.2}\text{Sr}_{1.6}\text{Ca}_{0.2}\text{Mn}_2\text{O}_7$), but a comparison with data provided by studies carried out on single crystals modifies this picture. If we extrapolate, at low temperatures, the performances of the manganese perovskites, whose T_C s are in the room temperature range, then it appears that $\text{La}_{1.2}\text{Sr}_{1.8}\text{Mn}_2\text{O}_7$ exhibits somewhat higher MR values [15]. A closer examination of this maximum MR leads to an interesting observation. This latter, for $\text{La}_{1.2}\text{Sr}_{1.8}\text{Mn}_2\text{O}_7$ and in all directions, is located right in the two-dimensional critical magnetic fluctuations regime (around $121 \text{ K} > T_d \approx 117 \text{ K}$, T_d standing for the lattice crossover temperature [8]), indicating that the dimensionality of the critical fluctuations influence the high-field MR to some extent. That such a maximum occurs in this temperature range agrees well with their lower relative thermodynamic stability. Several authors [16] have

explained why lower T_{im} yield higher maximum values of MR. But what our measurements on single crystals reveal is much deeper than a simple effect on T_{im} . In figure 3, we can note that for $\text{La}_{1.2}\text{Sr}_{1.8}\text{Mn}_2\text{O}_7$ ($\text{La}_{1.2}\text{Sr}_{1.6}\text{Ca}_{0.2}\text{Mn}_2\text{O}_7$), the resistivity drops by an order of magnitude going from 2 (1) below the insulator–metal transition along the [110] direction to 3 (3) in the direction perpendicular to the double-perovskite slabs (reflecting the way in which transport anisotropy evolves in this temperature domain (figure 2)). MR ratios obtained in this direction are consequently higher than those along [110], and hence than those of their single-crystalline three-dimensional homologues with identical T_C s ($\text{MR}_{\text{max}[001]}(8\text{ T}) \approx 1150$ for $\text{La}_{1.2}\text{Sr}_{1.8}\text{Mn}_2\text{O}_7$ and $\text{MR}_{\text{max}[001]}(8\text{ T}) \approx 1260$ for $\text{La}_{1.2}\text{Sr}_{1.6}\text{Ca}_{0.2}\text{Mn}_2\text{O}_7$). The non-magnetic insulating (La, Sr, Ca)O barrier does indeed make a contribution to the magnetoresistive effect. In passing, note also that this feature, for $T < T_{im}$, was not identified for powder specimens of similar compositions [17], because of the extrinsic complexity that their microstructure causes.

3.3. Low-temperature resistivity

At low temperatures, the resistivities measured without an applied field along [110] and [001] exhibit the same insulating behaviour, diverging logarithmically over a wide temperature range, typically 7–30 K (figure 5). In this temperature range, the transport anisotropy remains constant; this suggests a common charge transport mechanism within the bilayers and along the perpendicular direction, and not a two-dimensional weak localization. None of the resistivity experimental data below T_{min} could be fitted to a thermal activation law or the variable-range hopping model nor any power law. The best fit is achieved to a logarithmic function $\rho = a + b \ln T$, and this is somewhat puzzling. Indeed, the resistivities are likely to be too high to account for the weak localization. In particular, Ca-doped compounds possess a resistivity higher than that of $\text{La}_{1.2}\text{Sr}_{1.8}\text{Mn}_2\text{O}_7$ by two to four orders of magnitude, so one would rather expect a Mott law (Anderson insulator) to account for the resistivity increase at low temperatures. Such low-temperature resistivity increases have already been observed in transition metal oxides with perovskite structure such as LaNiO_3 and $\text{La}_{0.6}\text{Sr}_{0.4}\text{CoO}_3$ [18] and (La, Ca) MnO_3 [19], and are generally associated with weak-localization effects or electronic correlations [20]. However, in the particular cases of (La, Ca) MnO_3 [19], (La, Sr) MnO_3 and $\text{Pr}_{0.7}\text{Sr}_{0.3}\text{MnO}_3$ manganites [15], this low-temperature divergence does not occur in metallic single crystals and, so, one can rightly invoke some extrinsic origin due to microstructure.

Figure 5 suggests that in $\text{La}_{1.2}\text{Sr}_{1.8}\text{Mn}_2\text{O}_7$, the magnetic field affects only the constant a . According to Matthiessen's law, a consists of the sum of a residual resistivity (due to defects) and a magnetic one. Consequently, we are dealing with a classical MR that goes to zero with temperature. On the other hand, in $\text{La}_{1.2}\text{Sr}_{1.6}\text{Ca}_{0.2}\text{Mn}_2\text{O}_7$, it seems that the magnetic field influences both a and b , and so there would be some quantum corrections to the resistivity, providing the beginnings of an explanation for the higher MR values obtained at low temperatures ($\text{MR}_{[110]}(2\text{ T}) \approx 0.5$ for $\text{La}_{1.2}\text{Sr}_{1.6}\text{Ca}_{0.2}\text{Mn}_2\text{O}_7$ as against $\text{MR}_{[110]}(2\text{ T}) \sim 10^{-2}$ for $\text{La}_{1.2}\text{Sr}_{1.8}\text{Mn}_2\text{O}_7$ at 2 K). This particular MR emerges at low temperature when the relative contribution of the residual resistivity to the total resistivity prevails over the thermal scattering ones.

4. Conclusions

The close relations between magnetic and electronic properties in the $\text{La}_{1.2}\text{Sr}_{1.8-y}\text{Ca}_y\text{Mn}_2\text{O}_7$ ($0 \leq y \leq 0.2$) system have been given further support through detailed resistivity and MR measurements. The insulator–metal transition, which is reversible like the ferromagnetic one [8], occurs in all directions, if we exclusively rely on the resistivity slope sign criterion,

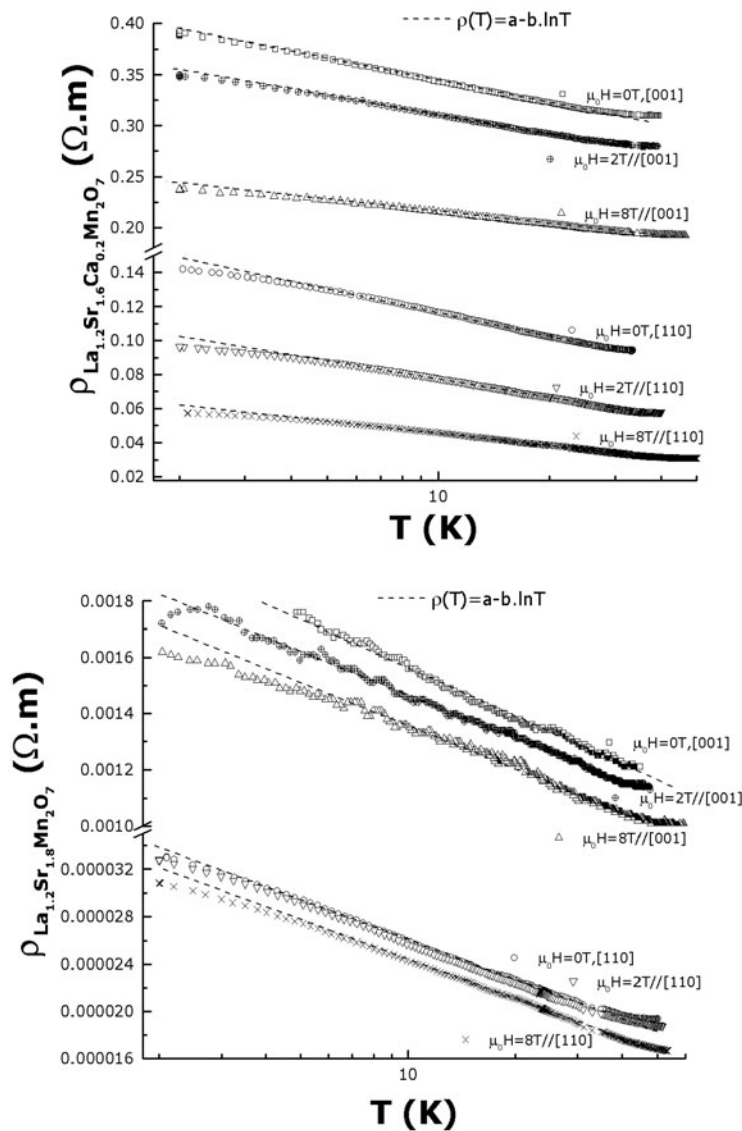


Figure 5. The logarithmic divergence of the resistivity at low temperatures under various fields for $\text{La}_{1.2}\text{Sr}_{1.8}\text{Mn}_2\text{O}_7$ and $\text{La}_{1.2}\text{Sr}_{1.6}\text{Ca}_{0.2}\text{Mn}_2\text{O}_7$, along the c -axis and $[110]$.

consistently with the three-dimensional nature of the ferromagnetic ordering. A further examination of the resistivity value reveals that metallicity is indeed poor and ‘rigorously’ established within the bilayered perovskite slabs, in agreement with the magnetic coupling anisotropy [12]. Quasi-two-dimensional correlations could account for the substantial high-field MR at room temperature as well as for the temperature dependence of the $\rho_{[001]}/\rho_{[110]}$ anisotropy transport ratio. The non-magnetic (La, Sr, Ca)O barrier was found to increase the high-field MR values, just below T_{im} , to above those of $\text{La}_{1.2}\text{Sr}_{1.8-y}\text{Ca}_y\text{Mn}_2\text{O}_7$ three-dimensional homologues. Finally, the intrinsic resistivity divergence at low temperatures and its field dependence have been specified and found to follow a logarithmic form.

Acknowledgments

M Velázquez wishes to thank his co-workers A Anane, M Compin and L Reversat, for outstanding technical support and 'know-how'. It is a pleasure to thank Dr M Aprili and Dr L Vasiliu-Doloc for fruitful and enlightening discussions, and Dr J P Doumerc for a critical reading of the manuscript. M Velázquez is also indebted to A F Santander-Syro and N Bontemps, from the Laboratoire de Physique du Solide, ESPCI, Paris, for making possible optical measurements on our single crystals.

References

- [1] Moritomo Y, Asamitsu A, Kuwahara H and Tokura Y 1996 *Nature* **380** 141
- [2] Kimura T, Tomioka Y, Kuwahara H, Asamitsu A, Tamura M and Tokura Y 1996 *Science* **274** 1698
Kimura T, Tomioka Y, Asamitsu A and Tokura Y 1998 *Phys. Rev. Lett.* **81** 5920
Li J Q, Matsui Y, Kimura T and Tokura Y 1998 *Phys. Rev. B* **57** 3205
- [3] Dessau D S, Saitoh T, Park C H, Shen Z X, Villeda P, Hamada N, Moritomo Y and Tokura Y 1998 *Phys. Rev. Lett.* **81** 192
Saitoh T, Dessau D S, Moritomo Y, Kimura T, Tokura Y and Hamada N 2000 *Phys. Rev. B* **62** 1039
- [4] Zhou J S, Goodenough J B and Mitchell J F 1998 *Phys. Rev. B* **58** 579
- [5] Argyriou D N, Mitchell J F, Potter C D, Bader S D, Kleb R and Jorgensen J D 1997 *Phys. Rev. B* **55** 11 965
Medarde M, Mitchell J F, Millburn J E, Short S and Jorgensen J D 1999 *Phys. Rev. Lett.* **83** 1223
- [6] Kubota M, Fujioka H, Hirota K, Ohoyama K, Moritomo Y, Yoshizawa H and Endoh Y 2000 *J. Phys. Soc. Japan* **69** 1606
Ling C D, Millburn J E, Mitchell J F, Argyriou D N, Linton J and Bordallo H N 2000 *Phys. Rev. B* **62** 15 096
- [7] Argyriou D N, Kelley T M, Mitchell J F, Robinson R A, Osborn R, Rosenkranz S, Sheldon R I and Jorgensen J D 1998 *J. Appl. Phys.* **83** 6374
- [8] Velázquez M, Revcolevschi A, Renard J P and Dupas C 2001 *Eur. Phys. J. B* **23** 307
- [9] Velázquez M, Haut C, Hennion B and Revcolevschi A 2000 *J. Cryst. Growth* **220** 480
- [10] We measured the far- and medium-infrared reflectivity ($30 < \sigma \text{ (cm}^{-1}\text{)} < 6000$) at room temperature for a $\text{La}_{1.2}\text{Sr}_{1.8}\text{Mn}_2\text{O}_7$ single crystal grown by us (see [9]), with Santander-Syro and Bontemps, at the Laboratoire de Physique du Solide of the ESPCI, in Paris. We also found $\hbar\omega_2 \sim 20$ meV and $\hbar\omega_1 \sim 43$ meV, in good agreement with the measurements at lower temperatures of
Ishikawa T, Kimura T, Katsufuji T and Tokura Y 1998 *Phys. Rev. B* **57** 8079
- [11] According to Vasiliu-Doloc L (2002 private communication), we can obtain a rough estimate of the Debye temperature from the cut-off wavelength for an acoustic phonon mode (the highest measured using neutrons in the $(0k0)$ planes), namely ≈ 20 meV; hence $\theta_D \sim 232$ K.,
- [12] Rosenkranz S, Osborn R, Mitchell J F, Vasiliu-Doloc L, Lynn J W and Sinha S K 2000 *J. Appl. Phys.* **87** 5816
- [13] Millis A J 2000 *Theory of CMR Manganites, Colossal Magnetoresistance Oxides (Advances in Condensed Matter Science vol 2)* ed Y Tokura (London: Gordon and Breach) p 53
- [14] Khazeni K, Jia Y X, Lu L, Crespi V H, Cohen M L and Zettl A 1996 *Phys. Rev. Lett.* **76** 295
- [15] Anane A 1998 *PhD Thesis* Paris VI University
Anane A 2001 private communication
- [16] Ramirez A P 1997 *J. Phys.: Condens. Matter* **9** 8171
- [17] Shen C H, Liu R S, Hu S F, Lin J G, Huang C Y and Sheu H S 1999 *J. Appl. Phys.* **86** 2178
Liu R S, Shen C H, Hu S F, Lin J G and Huang C Y 2000 *J. Magn. Magn. Mater.* **209** 113
- [18] Raychaudhuri A K 1995 *Adv. Phys.* **44** 21
- [19] Jaime M and Salamon M B 1999 Electronic transport in La–Ca manganites *Physics of Manganites* ed T A Kaplan and S D Mahanti (Dordrecht: Kluwer)
- [20] Lee P A and Ramakrishnan T V 1985 *Rev. Mod. Phys.* **57** 287